Electromagnetic therapeutic coils design to reduce energy loss

Przemyslaw Syrek[1], Mikolaj Skowron[1], Szczepan Moskwa[1], Wojciech Kraszewski[1] and Antoni Ciesla[1]

[1]*AGH University of Science and Technology, al. Mickiewicza 30, 30-059 Krakow, Poland*

Abstract. The article introduces the problem of power loss reduction in applicators used in magnetotherapy. To generate magnetic field whose distribution is optimal and to reduce the power loss, the authors establish a set of parameters to evaluate the model of device. Results make it possible to infer that the real power input necessary to operate the magnetic field generator properly may vary significantly depending on construction and localization. The issues raised in this paper should be treated as a basis for further discussion on the construction of applicators used, e.g., in Transcranial Magnetic Stimulation.

1 Introduction

Biological effects of low-frequency electromagnetic field on living organisms have been investigated for few decades. There is wide range of publications that show beneficial influence of EMF, i.e. accelerated tissue regeneration, reduced bone fracture healing time, pain relief, and the anti-inflammatory effect [1,2].

In the extremely low frequency band, both components of electromagnetic field and their influence the human tissues may be considered separately. Both components are used in a wide range of medical problems. Remotely supervised therapies are developed in many branches of medicine, e.g. related to the brain stimulation [3]. Since the fractures and general orthopedic injuries contribute to increase in sick absence from work by several percent, this aspect requires the use of available technical means. Therapy conducted remotely has many advantages: travel time related to rehabilitation is reduced to the barest minimum, whereas the duration of the session is in principle unlimited. In this context, the energy saving problem arises. While searching patent databases, one may find numerous claims concerning magnetic field control systems and power supply methods.

The present article presents the problem of energy loss reduction in order to extend the continuous operation of the portable magnetic field applicator. The energy loss is results from four causes: the energy source itself, the converter and the impulse generator, the anatomical structures absorbing the energy, and the final cause is within the applicator's winding. The first two are beyond the scope of our consideration. Human tissues and their electric conductivity combined with current range induced by devices produce a negligible energy level, especially in the extremely low frequency band. Even the energy absorbed by human tissue, which is an inherent consequence of hyperthermia, could be omitted, if we take into account tissue parameters like heat capacity, density, and the volume under treatment [4].

Therefore, a variety of stimulators coil shapes are considered in order to focus or ensure the uniformity of electric or magnetic field [5]. The coil winding design should take into account energy efficiency as well. The results, which were obtained using evolutionary strategy, are presented for one of many objective functions that may be adopted, which depend on requirements imposed on field distribution.

2 Outline of the problem

In order to avoid the multi-criteria optimization, the problem of the device construction cost is omitted. The applicator winding is to generate a time-varying magnetic field. Depending on the therapeutic requirements, only the same magnetic component of the EMF or indirect utilization of magnetic field is required for generation of an electric field, and thus the eddy currents in the tissues of the body under treatment [6].

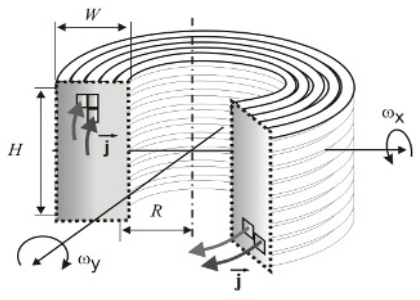

Figure 1. Real valued parameters for applicator.

[a] Corresponding author: syrekp@agh.edu.pl

2.1 Magnetic field generator

The selected aspects of energy loss reduction are considered. The first problem is to specify the relation between resistance and reactance of applicator winding. In the low frequency band, self-inductance, and hence the reactance, is a hundredth part of resistance. Therefore, the dominant is real power compared to the reactive power, despite the fact that the reactive power may be relatively easily and cheaply compensated.

The magnetic field distribution, especially its absolute value, depends on a number of factors: the shape of the winding and its construction (or the modeling of curve representing the wire) in general, wire length, cross sectional area, current supplied to the device. While the winding resistance increases linearly with its length, the energy loss grows as well. In turn, in the linear model, the magnetic field at each point in space is proportional to the current, while the power loss is proportional to the square of the current. Here occurs the main problem concerning the construction of the applicator, which is related to the compromise between the applicator winding and amperage. It follows that, in order to reduce losses, the increase in the length of the applicator is the right direction (successive layers and turns of the winding, fig.1), whereas the current should be reduced. Unfortunately, this approach has its own limitation. Adding another layers means that they are farther away from the target points of its influence, and the decrease in the magnetic field can be assumed to be equal to the square (or almost square) of the distance.

The magnetic induction is calculated using the line integral:

$$\mathbf{B} = (\mu_0/4\pi) \int_V (\mathbf{j}_S \times \mathbf{r})/|\mathbf{r}|^3 \, dV \qquad (1)$$

where $\mathbf{j}_S$ represents current density, $\mathbf{r}$ is the vector pointing from the target point to dV – infinitesimal portion of the coil.

2.2 Applicator parameters

In [7], authors propound the method of placing turns within the coil to concentrate the magnetic and electric field with the minimal energy cost.

Since the magnetic field diminishes with nearly the square of distance, arbitrary specification of the location of applicator relative to the body seems to be inadequate and may significantly disrupt the results of power loss. Thus, the set of parameters for position of the applicator is not to be neglected. In the case of solenoid applicator, five parameters are enough to provide any position [8]. Thus, the best location will be ensured in the context of adopted cost evaluation. We do not distinguish between individual turns of the applicator coil, but replace them with the current density in the cross-section. This method makes it possible to use continuous optimization and real-valued parameters for dimensions and position of the applicator. The parameter j_{RMS} is the RMS of absolute value of current density vector in the wire.

Eight real valued variables describe the vector that represents the applicator:

$$\mathbf{x} = [\, R \; W \; H \; \omega_X \; \omega_Y \; x \; y \; z \,]^T \qquad (2)$$

These parameters are used to describe each individual in the populations used in the evolutionary optimization process. The first three represent the dimensions of the device, next two represent applicator rotation around the axes of the coordinate system and last three correspond to its position in any direction. Table 1 introduces limits for each parameter. The search space is the hypercube in 8 dimensions.

Table 1. Limits for applicator parameters.

Variable	Lower bound	Upper bound
R	0.005 [m]	0.080 [m]
W	0.010 [m]	0.050 [m]
H	0.010 [m]	0.016 [m]
ω_X	0 [rad]	2π [rad]
ω_Y	0 [rad]	π [rad]
x	–0.2 [m]	0.5 [m]
y	–0.2 [m]	0.5 [m]
z	0 [m]	1.0 [m]

2.3 Applicator evaluation

Since the ferromagnetic materials are excluded, and a constant electric conductivity of copper wires is assumed, the model is linear. Due to linearity, the current density j may be omitted in the set of control parameters. During the cost evaluation, the magnetic (or electric) field may be obtained at the arbitrary level of j_{RMS} conventionally equal to 1 A/mm^2. Then, the current density should be rescaled for the sake of the field at the required level:

$$j_{RMS} = (B_{REQUIRED}/B_{OBTAINED}) \cdot 1 \; [\mathrm{A/mm^2}] \qquad (3)$$

Whereas the power loss:

$$P_{TOTAL} = (j_{RMS}^2/\gamma_{CU}) \cdot V \; [\mathrm{W}] \qquad (4)$$

where: γ_{CU} –electric conductivity of copper, V – volume of conducting elements of an applicator.

The quantity (4) is the measure of cost assigned to each individual in the evolutionary strategy for optimization of the title device.

3 Optimization process

Some aspects of optimization process i.e. real-valued parameters of the device, search space boundaries and cost measure definition were presented in the above sections.

To determine the location of target points and to remove and hence "to hollow" the search space, the numerical model of human was used (fig. 2). This is the Virtual Family Model [9], which represents the patient. Exactly, Ella, a 26-years old female model (1.66 m height, 57.3 kg weight) is such a virtual patient. The available models are made of 0.5, 1, 2 and 5 mm voxels. The iso2mesh free library was used to generate 3D meshes on the basis of the voxel [10], and the mesh was developed using generate tetrahedral mesh generation software – TetGen [11].

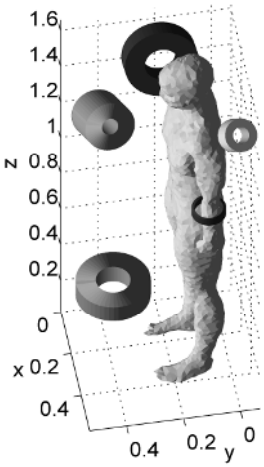

Figure 2. An example set of applicators to evaluate, and the surface for collision detection.

3.1 Violation factor

The position of the applicator is constrained, which results from collision between human body and the device. The solution beyond hypercube as the feasible region, is simple to transform and put at least at the boundary. In the event of a collision with body model, the case becomes more complicated. Both violation factor assignment and restoration of solution point on the border between the patient model and search space are of high computational complexity even when referring to the EMF problems and their calculation costs. Therefore, evolutionary strategies involving the real-valued penalty due to violation degree are omitted. Instead of tolerating a group of individuals slightly in excess of the feasible solution area (and use the exterior penalty factor) to take advantage of an attractive part of their genotype, we propose the elimination of such solutions. It involves the avoidance of unnecessary cost function evaluations.

3.2 Evolutionary strategy

A description of the applicator using real variables allows for a wide variety of evolutionary strategies.As it can be implied from the no free lunch theorem [12], every problem should be matched a strategy that best copes with it. Especially in the case of field problems, where an assessment is usually computationally complex.

Overview and tests of possible strategies pointed to the necessity of elimination. The strategies to be eliminated are the ones that involve a degree of violation, i.e. precise collision detection. Due to the computational complexity of such an approach, these concepts are beyond the area of interest. Imperial Competitive Algorithm is found out to be ineffective when up to five variables may affect finding infeasible chromosome.

The other strategy, Differential Evolution, has a great potential when it comes to seeking the position of the applicator, even if we include the above mentioned problem of removing solutions involving a collision with a body, while the 3 variables responsible for the construction of the applicator and the narrow range of their values makes this method inadequate.

The next aspect is the stop criterion. In [13], $N \cdot 10^5$ candidate solutions evaluation is suggested, where N is the problem dimension. Both the tests of strategies (in terms of population size, reproduction and mutation ratio) and the results of optimization presented below, were conducted through 20000 cost functions evaluations. Instead, each result was obtained by 30 repetitions to control the repeatability of results. The strategy that has eventually been adopted used the population of 150 individuals picked using elitist selection, and the genotype has been enhanced by parameter of mutation strength that evolves with the population [14] to strengthen exploitive abilities of population.

4 Results and discussions

Figure 3 presents the best individual (the best solution to the problem) and the device modeled by it optimized on the basis of the above mentioned for tibia bone piece, 60 mm in length. Applicator induces magnetic field of at least 1 mT within the bone fragment, the real power needed is in this case equal to 0.48 mW with the coil length of 1198 meters.

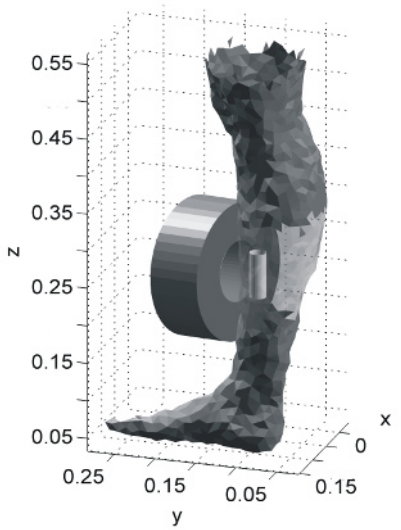

Figure 3. Applicator for therapy of a tibia bone fragment.

Results of optimization are presented in Table 2 and Fig. 4. Applicators and their optimal parameters were obtained for a wide range of magnetic induction that was required within part of tibia bone. A graph on a logarithmic scale shows that power and current increases significantly with the magnetic field specified. The coil length is almost constant. The *W*-parameter, which corresponds to turns of winding, reaches the upper bound of its limitations (parameters marked with * in the tab.2, to stand out feasible solution border) in each case. Otherwise, the *H*-parameter (the possible number of coil layers) increases with the magnetic induction needed. The very important observation on this parameter is that the optimal solution optimal does not converge to its upper bound, what let decrease current supplied to the coil. This conclusion results from the manner the magnetic field diminishes within the target space when the next layers are added. This aspect the fair possibilities to reduce energy consumption by this category of devices.

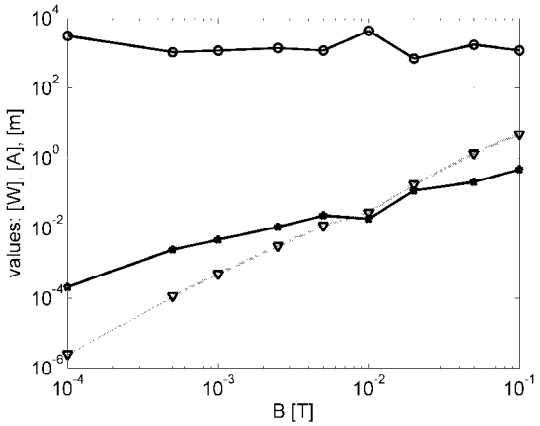

Figure 4. Results of optimization aimed at a variety of magnetic induction values. Plots for: real power (triangles), current for 1 mm^2 wire (stars), coil length (circles).

5 Conclusions

As a result of the simulations, it was confirmed that not all parameters of the applicator model must be at the upper boundary of the solution space (table 2). On the contrary, further enhancement of certain parameters would result in a faster power loss growth than the component of the magnetic field, which results from the distance of the successive turns of the device from the target points – space to focus the field.

An important observation is that larger applicators may also be used for mobile application. In this case it is limited by the possible discomfort of the patient, but from an energy point of view, it is an attractive construction. Further considerations also need to take the cost of construction that includes the wire and the applicator housing costs into account. The problems presented here should be treated as a basis for further discussion on the construction of applicators used, e.g., in Transcranial Magnetic Stimulation, where it is desirable to achieve the highest value of components of the electric and magnetic field in certain subspaces of the brain, and the technical solutions currently used in this process involve pulse generation using the superconductivity. These solutions are at the limit of modern technology.

Table 2. Results of optimization for real power loss (feasible solution upper bound marked with *).

B **[mT]**	***P*** **[mW]**	***l*** **[m]**	***R*** **[m]**	***W*** **[m]**	***H*** **[m]**
0.5	0.117	1081	0.028	0.049*	0.063
1	0.486	1198	0.028	0.049*	0.071
5	11.84	1203	0.029	0.049*	0.070
50	13570	1771	0.035	0.050*	0.092

References

1. K. Sieron-Stoltny, L. Teister, G. Cieslar, D. Sieron, Z. Sliwinski, M. Kucharzewski, A. Sieron, Biomed Res. Intern., 896019 (2015)
2. A. Fathi Kazerooni, M. Rabbani, M.R. Yazdchi, IFMBE Proceedings **35**, 458–462.(2011),
3. L.E. Charvet, M. Kasschau, A. Datta, H. Knotkova, M. C. Stevens, A. Alonzo, C. Loo, K.R. Krull, M. Bikson, Frontiers in Systems Neuroscience, **9** (2015), 26, 1-13.
4. E. Kurgan, P. Gas, Przegl. Elektrotech. (Elect. Rev. **87(12b),** 103-106 (2011).
5. D. Zhi-De, S.H. Lisanby, A.V. Peterchev, Brain Stimulation **6,** 1–13 (2013).
6. A. Krawczyk, A. Miaskowski, E. Lada-Tondyra, Y. Ishihara, Przegl. Elektrotech. (Elect. Rev.) **86(12),** 72-74 (2010)
7. L. Darabant, M. Plesa, D.D. Micu, D. Stet, R. Ciupa, A.Darabant, IEEE Transact. on Magn. **3**, 1690-1693 (2009),.
8. A. Ciesla, P. Syrek, Przegl. Elektrotech. (Elect. Rev.) **88(**12b**),** 124-127 (2012).
9. A. Christ, W. Kainz, E.G. Hahn, K. Honegger, M. Zefferer, E. Neufeld, W. Rascher, R. Janka, W. Bautz, J. Chen, B. Kiefer, P. Schmitt, H.P. Hollenbach, J.X. Shen, M. Oberle, D. Szczerba, A. Kam, J.W. Guag, N. Kuster, Phys. in Med. and Bio. **55** (2), N23-N38 (2010).
10. Q. Fang, D. Boas, Proceedings of IEEE Intern. Symp. on Biomed. Imag., 1142-1145 (2009).
11. Si Hang, ACM Trans. on Math. Soft. **41** (2), (2015).
12. D.H. Wolpert, W.G. Macready, IEEE TransEvolComp **1**,67-82 (1997).
13. K. Opara, J. Arabas, J. of Telec. and Inf. Techn., **4** 73-80 (2011),.
14. H.G. Beyer, H.P. Schwefel, Nat. Comp. **1,** 3–52 (2002).